Estuarine, Coastal and Shelf Science 80 (2008) 153–160

Contents lists available at ScienceDirect

Estuarine, Coastal and Shelf Science

journal homepage: www.elsevier.com/locate/ecss

Observation of internal tidal currents in the Kaoping Canyon off southwestern Taiwan

Y.H. Wang [a], I.H. Lee [b,*], J.T. Liu [c]

[a] Institute of Applied Marine Physics and Undersea Technology, National Sun Yat-sen University, Kaohsiung 804-24, Taiwan ROC
[b] National Museum of Marine Biology and Aquarium, Pingtung 944-50, Taiwan ROC
[c] Institute of Marine Geology and Chemistry, National Sun Yat-sen University, Kaohsiung 804-24, Taiwan ROC

ARTICLE INFO

Article history:
Received 26 October 2007
Accepted 18 July 2008
Available online 30 July 2008

Keywords:
internal tides
Kaoping Canyon
phase velocity
isotherm displacement

ABSTRACT

Internal tidal currents and associated water-mass displacements were investigated during multiple cruises in the Kaoping Submarine Canyon off southwestern Taiwan. Observations from both moored and shipboard Acoustic Doppler Current Profilers and hydrographic casts were conducted along the canyon. The velocity data showed that in the lower layer the major axis of the tidal currents aligned with the orientation of the canyon, and currents moved up-canyon during flood and down-canyon during ebb. The vertical-phase shift and amplitude of the currents indicated that the semidiurnal internal tide dominated with intensity increasing with depth toward the canyon head. Tidal energy was channeled from the shelf landward with a beamlike internal wave, guided by bottom topography. The estimated phase velocity was 1.4–1.7 m s^{-1}, based on normal mode analysis and the phase lag between sampling stations. Empirical orthogonal function analysis of hydrographic profiles confirmed that the first mode (M_2 internal tide) explained 70% of the total variance. The strong convergence of internal tidal currents near the canyon head during flood may play an important role in the daily migration of cherry shrimps, which burrow along the canyon wall.

1. Introduction

Kaoping Submarine Canyon (KPSC) is located southwest of Taiwan (Fig. 1). It begins at the mouth of the Kaoping River, crosses a 20-km narrow shelf, then merges into the northern Manila Trench. The canyon is a major conduit for river-borne and marine materials. Based on the distribution of coprostanol (a tracer for human waste) inputs of 20 years, Jeng et al. (1996) showed that the concentration was highest at the river mouth and decreased to 1% at the shelf break. However, the concentration remained high at the bottom of the meandering canyon 35 km from the canyon head. Huh et al. (in press), on the basis of the sediment budget and the presence of short-lived ^{7}Be and nonsteady-state distribution of low levels of ^{210}Pb in sediments, suggested a rapid transport of sediments from the Kaoping River's mountainous watershed via the canyon to the abyssal plain and the Manila Trench in northern South China Sea.

Tidal currents generally dominate the flow field in many submarine canyons, and the internal tides may be an order of magnitude more energetic than the barotropic tidal currents (Kunze et al., 2002). The internal tidal current-associated water–mass displacements may have major effects on the sediment transport, as suggested by McPhee-Shaw et al. (2004). In Monterey Canyon (MC), off California, for example, Petruncio et al. (1998, 2002) reported that the internal tides were a major feature and the baroclinic currents were an order of magnitude greater than the estimated barotropic tidal currents. The internal tide-induced isopycnal displacement was found to have amplitudes up to 50 m. Xu et al. (2002) showed that the tidal currents dominated at all sites in MC and that the up-canyon and down-canyon currents were closely correlated with the timing of tides. The bottom intensification of tidal currents plays an important role in raising the near-bottom shear stress that bottom sediments often are resuspended. On the east coast of the United States, Hotchkiss and Wunsch (1982) reported that the vertical stratification in Hudson Canyon made easier the generation of internal tides, and the narrowing and steering action of submarine-canyon topography significantly enhanced the current speed.

The KPSC's subtropical location and persistent condition of warm water (above 25 °C) in the upper layer and cold water (below 12 °C) in the lower layer creates strong stratification. The internal tide is hypothesized to be easily generated and amplified owing to the strong density interface. The meandering "S" shape of the KPSC may further complicate the intensity of the flow. Few reports are available for the currents in this canyon because of the heavy trawling of fishing boats, which endangers instrumentation

* Corresponding author.
E-mail address: ihlee@nmmba.gov.tw (I.H. Lee).

0272-7714/$ – see front matter © 2008 Elsevier Ltd. All rights reserved.
doi:10.1016/j.ecss.2008.07.016

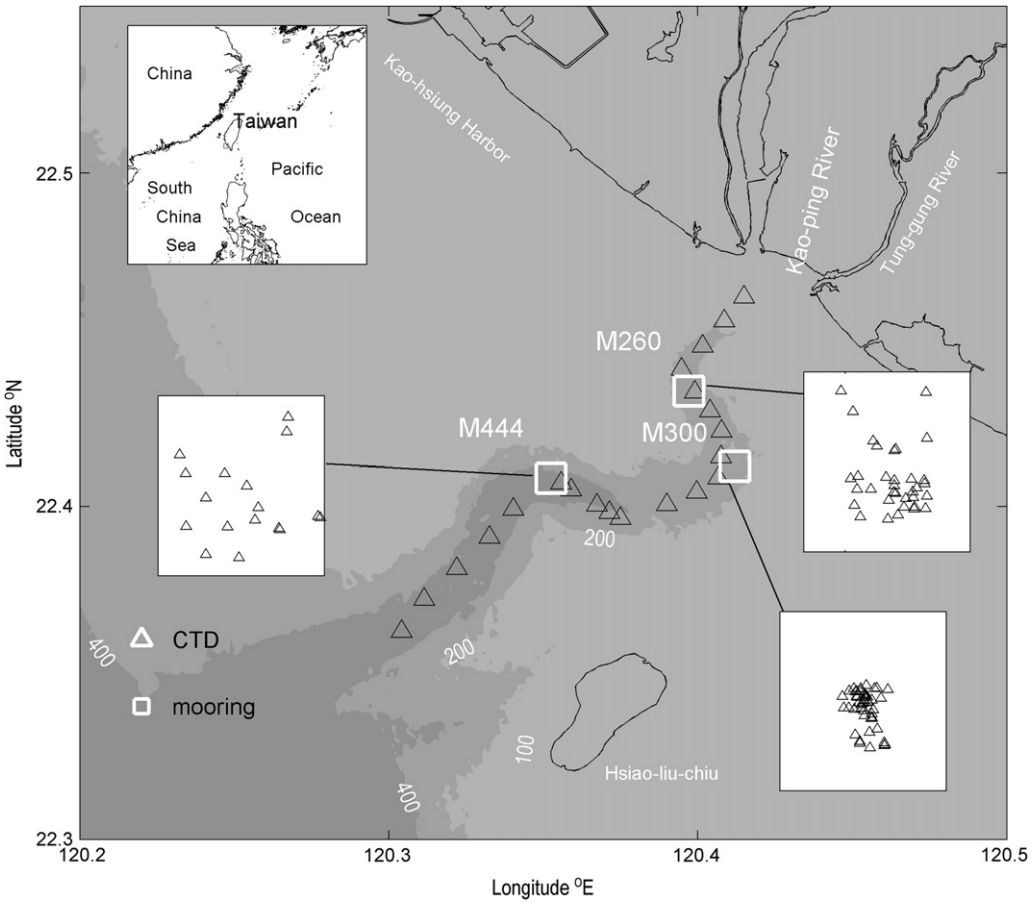

Fig. 1. Bathymetric map of the study site, showing a unique physiographic setting with a river estuary connected to a submarine canyon in a collision margin of arc and continent off southwestern Taiwan. White rectangles show mooring locations and black triangles show CTD stations. Hourly CTD profiles were conducted at the deepest part of the canyon near the moored stations when the research vessel was on station guarding the mooring.

deployment. This study, based on multiple cruises of measured current and density profiles along the canyon, is an attempt to quantify the amplitude of internal tides, their phase speed, and the possible effects of bends in the channel on them.

2. Field observations

The shipboard and moored Acoustic Doppler Current Profilers (ADCP) and the CTD were deployed during three cruises of the R/V Ocean Research 3 (OR3); the stations are indicated in Fig. 1. The first mooring (M444) was deployed on 13 December 2004. Two ADCPs (RDI WH 300, one upward looking and one downward looking) were mounted at mid-depth (200 m) in 444 m of water (Fig. 2). The mooring line tilted slightly because of drag by strong currents, resulting in an average of 30 m of vertical swing movement. The records from the pressure sensor in the ADCP were used to correct the depth of current measurements. The moored ADCPs recorded flows between 100 and 320 m, with a 2 m vertical resolution at 1 min time intervals. A total of 19 hourly CTD casts were collected on 13 and 14 December while the vessel was guarding the mooring. The measured parameters of the CTD profiling included temperature, salinity, depth, chlorophyll, dissolved oxygen, pH, PAR and light transmission.

On 14–17 December 2004 the OR3 vessel cruised along the main axis of the canyon for velocity surveys using the shipboard ADCP, sampling at 2 min intervals with 4 m of vertical resolution. A total of 30 repeated transects were occupied in 3 days. In one transect, 21 CTD casts were conducted evenly along the canyon (Fig. 1) in 6 h (940–1600 on 16 December) to observe the spatial variation of water density. Two fishing boats were hired to take turns guarding the mooring when OR3 left M444, but even this extra measure was unable to fend off the trawlers. The deployment was originally intended to be for a month-long period, but it was terminated after

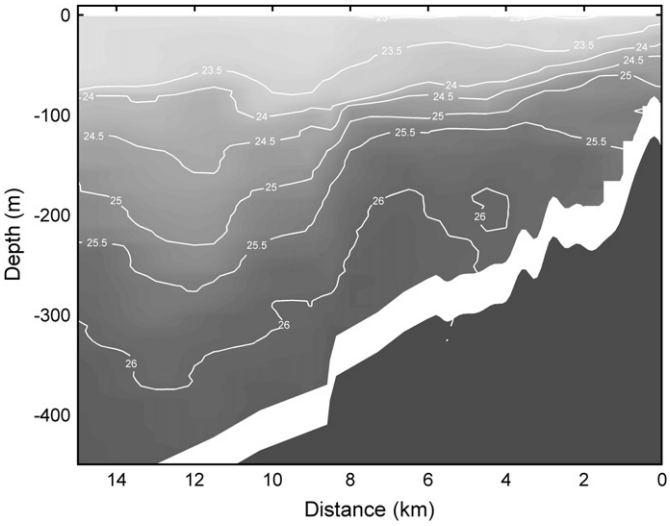

Fig. 2. Along-channel distributions of water density (sigma-t), based on CTD observations (indicated by 21 triangles in Fig. 1). The x-axis is the stretched distance of CTD stations, starting from the canyon head. The depth of the pycnocline decreases shoreward from 100 to 50 m. The density-induced reduced gravity, g', has a value of $\sim 0.03\ \mathrm{m\ s^{-2}}$. The smooth bottom topography indicates a steep slope near the canyon head ($\sim$1.5 km) and small humps down-canyon.

1 week when the mooring was entangled with a trawling fishing net. There were also 23 temperature loggers evenly mounted on the mooring line. Those data were not reported here owing to the data gaps caused by trawling loss of the loggers.

In two additional cruises the OR3 was stationed at M300 and M260, respectively. These operations involved long hours of CTD casts for the study of the water–mass displacement. The hydrographic data at mooring M300 were collected from 23 to 27 May 2005 in the middle section of the canyon. On this cruise a total of 69 CTD casts were obtained hourly in the deep canyon of 290–320 m (the ship might have drifted slightly by flood and ebb currents). A third experiment was carried out on 27 and 28 August 2006, when the OR3 was stationed in water 260 m deep near the head of the canyon. A total of 33 CTD casts were obtained at hourly time intervals on this cruise. Bottom-mounted ADCPs were deployed at M300 and M260 during the two OR3 cruises. The raw data resolution was 2 m in depth and every 5 min time intervals. Combined moored and shipboard ADCPs were used to reveal the flows in the upper layer (<300 m). All of the time series data were referenced to the 0 h of 1 January 2004, which makes it easy to compare the internal tidal-phase variations.

3. Baroclinic tidal flows

To reveal the characteristics and spatial variability of the surface tides, harmonic analyses were performed on 2 years of hourly sea-level data from Hsio-liu-chiu Island (Fig. 1). The mean tidal range for the area was about 1 m. The major tidal constituents were S_2 (0.14 m), M_2 (0.28 m), K_1 (0.28 m), and O_1 (0.21 m), which accounted for 90% of the variance. To get an idea of the along-canyon tidal propagation, we compared sea-level variation at Hsio-liu-chiu with month-long simultaneous measurements at the mouth of the Kaoping River. Harmonic analysis showed that the dominant M_2 amplitude had a negligible difference (0.02 m) between these two tide stations. The phase, however, showed a 29-min difference. The tidal wave appears to propagate from offshore toward the river mouth over the canyon.

A snapshot of the isopycnal distribution along the canyon is depicted in Fig. 2. The data were based on 21 CTD casts taken evenly along the canyon (Fig. 1) in 6 h, centered at high tide; the survey started near the canyon head when sea level was rising. The isopycnals were elevated below 100 m, which suggested a lower layer of cold water being pushed into the canyon. Then, at the middle section along the canyon, the profiles were compressed when sea level was highest. During the next 3 h the CTD stations in deep water were occupied when sea level was falling. The isopycnal showed a depression, suggesting that warm water was being drained from the canyon. There was a strong density gradient near 100 m, with the depth of the interface decreasing shoreward. The reduced gravity, g', was $\sim 0.03\ \mathrm{m\,s^{-2}}$. Thus the physical environmental setting favors generation of internal tides in the KPSC.

Fig. 3 shows the tidal-current ellipse of the two major constituents (M_2 and K_1), derived from the harmonic analysis of 7 day measurements at mooring M444. The dominant tidal constituent was M_2, and the amplitude increased with depth. Hotchkiss and Wunsch (1982) suggested that the wave energy can become trapped in a canyon owing to reflection off the canyon wall. Also, the canyon walls tend to converge with depth, enhancing the flow. Bathymetric measurements indicate that the cross-sectional distance of the canyon at M444 decreases from 3080 to 1650 m at depths of 180 and 320 m. The M_2 tidal currents were amplified from 0.21 to $0.58\ \mathrm{m\,s^{-1}}$ at these two depths; this is a threefold increase of speed where the cross-section width reduced by one-half. The diurnal (K_1) tidal currents were much smaller. No data were available above 100 m and below 330 m owing to the limited range of ADCP, which was moored at mid-depth (200 m) in 444 m of water.

In addition to the mooring data, along-canyon flows (measured with shipboard ADCP using RDI 150 kHz in 30 repeated transects on 14–17 December 2004) were illustrated by stick diagrams (Fig. 4).

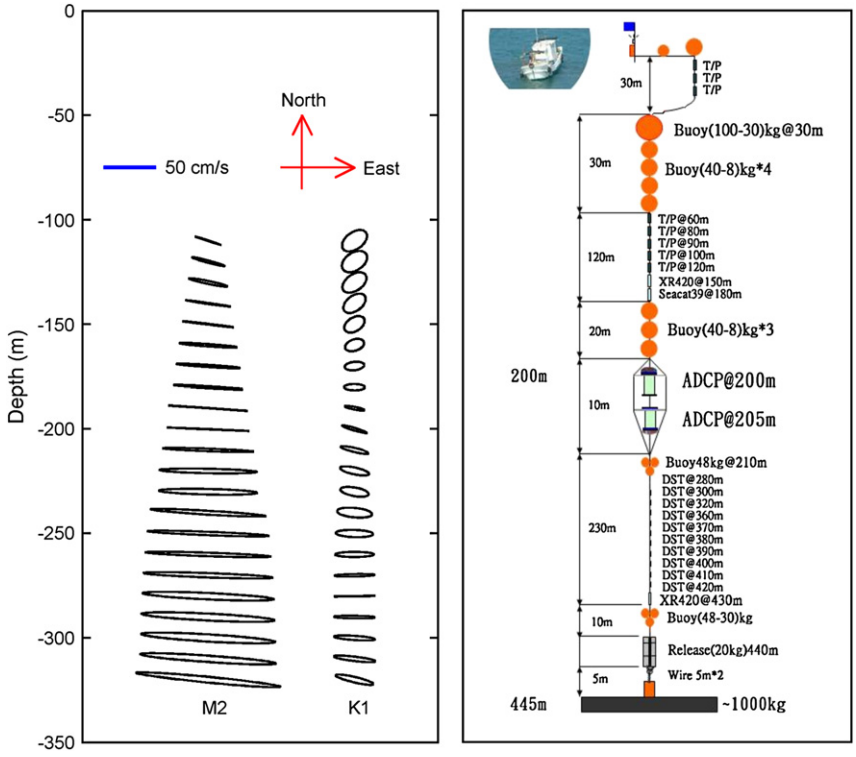

Fig. 3. Tidal ellipses (left) of M_2 and K_1 constituents derived from harmonic analysis of ADCP data from a mooring (right) at station M444. The dominant tidal constituent is M_2, and the amplitude increase with depth suggests that the wave is bottom-trapped in the KPSC.

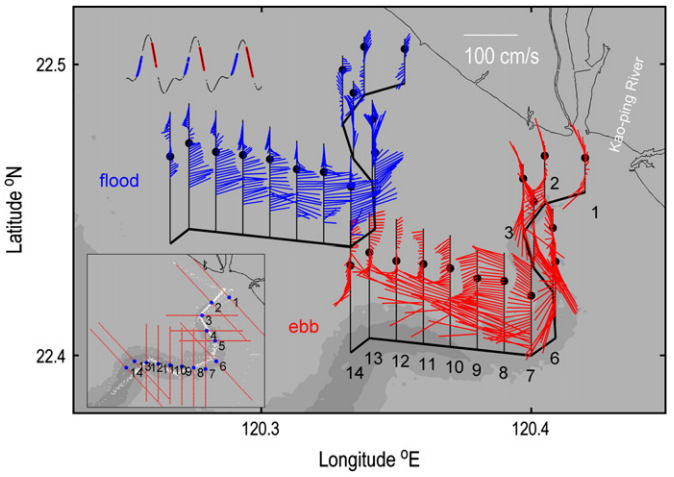

Fig. 4. Stick diagrams showing typical along-canyon flows of flood (upper left) and ebb (lower right) currents. Lower left inset indicates the cruise tracks (small dots) and shelf break (large dots) of each cross-canyon section. The sharp edges of the canyon rim were picked manually at each cross-canyon depth profile (not shown). Flow within the canyon is bottom-trapped and is down-canyon during ebb and up-canyon during flood. Flow patterns in the upper layer above the canyon rim are complicated and can be divided into sections according to the turns of the canyon axis.

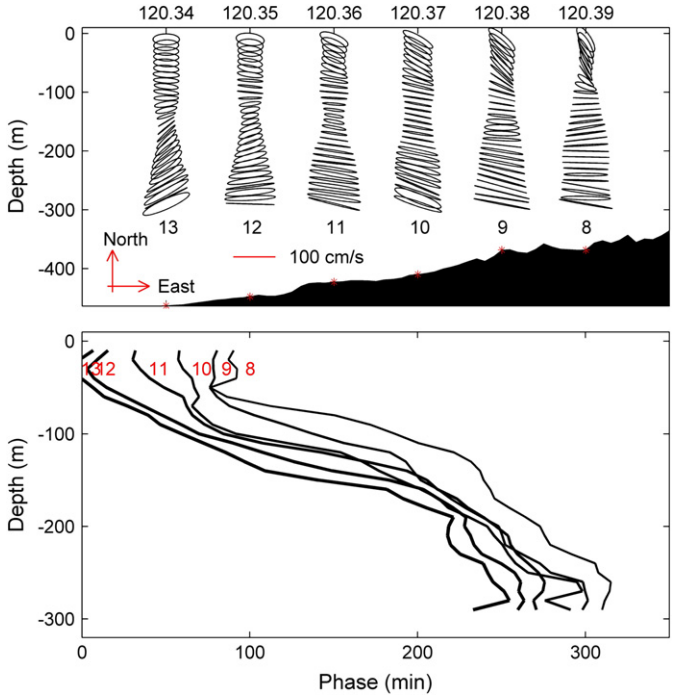

Fig. 5. M_2 tidal ellipse (top) and phase (bottom) for along-canyon flow. Station locations are shown in Fig. 4. The upper layer flow is basically barotropic with little vertical variation. The flow in the canyon, however, is baroclinic, with vertical-phase lags and phase lags among stations. The tidal amplitude increases downward, and the minimum flows center at 160 m for station 13 and 90 m for station 8.

These data cover the upper layer (300 m). The ADCP data were processed under standard data quality control (Wang et al., 2004) to remove outliers. The screened data were plotted to show the flow patterns of flood and ebb. Each stick in Fig. 4 represented an average of a 10 m vertical range and certain number of profiles included in the three segments of increasing/decreasing sea level (at Hsio-liu-chiu Island) as indicated on the inset plot. The depths of the canyon rim were identified at each cross-canyon section (lower left inset in Fig. 4) manually by viewing the depth profiles. Two distinct flow patterns emerged, according to the vertical variations in the flow direction. Flows within the canyon are down-canyon during ebb and up-canyon during flood. The velocities increased with depth, regardless of the orientation of the canyon axis. Flows above the canyon rim were complicated but appeared to respond to the orientation/turns of the canyon axis. The turning of flow directions at different locations suggested that currents over the canyon rim had different time lags with the phase of tidal elevation.

Harmonic regression was performed for the semidiurnal frequency (M_2), using data from the 30 transects conducted over 3 days, on stations 8–13 marked in Fig. 4. The six locations were spaced 1.1 km apart in a line along the main axis of the canyon. The data were divided spatially into grids within 1 km of the radius in the horizontal direction and 10 m in the vertical direction. Fig. 5 shows the ellipse and phase of the semidiurnal tide for the along-canyon flow. The M_2 tidal current ellipses were similar to those of M444, with the amplitude increasing with depth. The phase changes indicated that the upper layer flow was basically a barotropic tide with little vertical-phase variation. In contrast, the flow in the canyon was a baroclinic tide with 2 h or more of vertical-phase lag centered at 150 m (bottom panel in Fig. 5).

The enhancement of energy propagating up-canyon was not only guided by the isopycnal but also by the along-channel bottom slope (Petruncio et al., 1998, 2002). The linear-phase increase with depth seen in Fig. 5 suggests the existence of a beamlike internal wave propagating landward. The beam angle can be estimated by locating depths of a given phase at different stations at a distance (Petruncio et al., 1998). For example, a phase lag of 2 h occurred at 80 and 150 m between stations 8 and 13, respectively. The horizontal distance between the stations was 5500 m, and the slope of the wave beam was ([150–80]/5500) 0.0127, which corresponded to an angle of 0.73°. This slope was almost parallel to the bottom ([460–370]/5500) 0.0164, which corresponded to an angle of 0.94° between stations 8 and 13. These parallel slopes suggested that the wave beam was guided by the bottom topography. The phase velocity (C_p) can be approximated (Gill, 1982) using vertical normal mode analysis: $C_p = [g' h_1 h_2/(h_1 + h_2)]^{0.5}$. For example, for station M444 the reduced gravity, g', had a value of about 0.03 m s^{-2}, and the depths of the upper (h_1) and lower (h_2) layers were 150 and 250 m, respectively. Thus the estimated phase velocity was 1.7 m s^{-1}. For a shallow station with decreasing water depth ($h_1 = 100$ m, and $h_2 = 200$ m), the phase velocity decreased to 1.4 m s^{-1}.

4. Vertical displacement of canyon waters

Flow and density variations at station M300 (upper panel) and M260 (lower panel) are shown in Fig. 6, from combined shipboard and moored ADCP data. The isopycnal depths were constructed from the CTD profiles. Basically, the fluctuations of isopycnal depths matched well with the isotherms, showing that the density change was due to vertical displacement of water with stratified temperatures. The isotherm (or pycnocline) and flow both fluctuated with the semidiurnal (M_2) period. The amplitudes of isotherm fluctuation reached, respectively, 80 m at M300 and 70 m at M260, which corresponded to crest-to-trough displacements of 160 and 140 m. The onsets of landward and seaward flows were related to the increase and decrease in sea levels. The cold water was at the end of the flood current, and the peak temperatures were at slack tide. The up-canyon flow led the density maximum by about 3 h. The flow and temperature were about 90° out of phase, which suggested the existence of a standing wavelike motion at the head of the canyon. Similar reflections of internal tides were reported at Upper Loch Linnhe of Scotland (Allen and Simpson, 1998) and the outer continental slope of northern California (McPhee-Shaw et al., 2004).

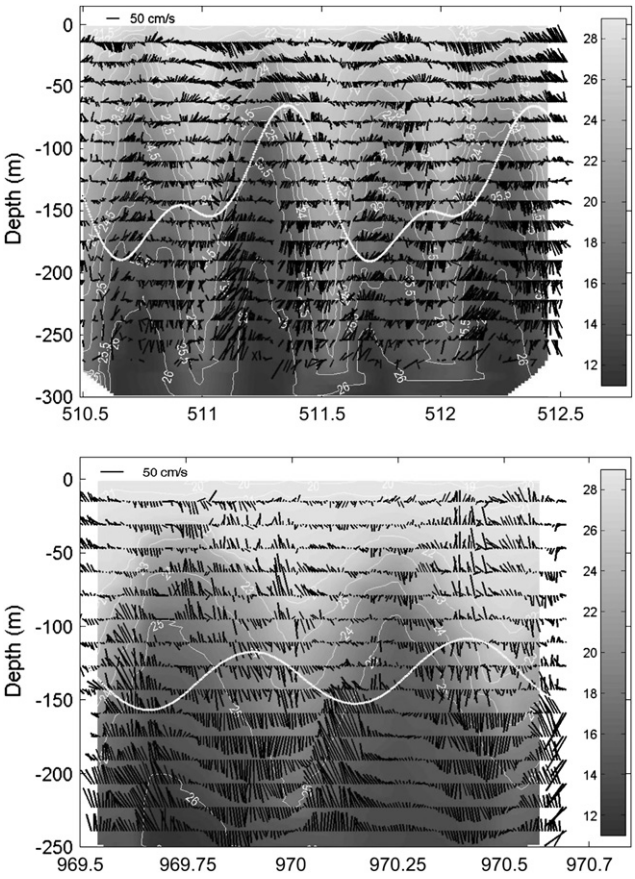

Fig. 6. Plots of CTD data with flow (stick) superimposed, based on moored data at station M300 (upper panel) and M260 (lower panel), with the *x*-axis indicating Julian days referenced to the 0 h of 1 January 2004. Flow sticks are a blend of shipboard and moored ADCP data. The temperature is indicated by the gray scale, and the white lines show the isopycnal (sigma-*t*) depths. The exaggerated sea level (thick line) from Hsio-liu-chiu Island is included to show the phase of the internal tidal current.

The hourly density profiles, based on CTD measurements from stations M444, M300, and M260, are plotted in Fig. 7. The minimum and maximum depths of the thermocline are illustrated by circles and dots. The time spans between large changes in the vertical density gradient were 6, 7, and 13 h for stations M444, M300, and M260, respectively, which indicates the dominance of M_2 tidal flow (the last one, 13 h, could have been two cycles). The vertical displacements of the isotherm were about 200, 160, and 140 m from the deep to the shallow stations. The displacements became less toward the canyon head. This was because the mixed-layer depth (pycnocline based on along-canyon CTD data) was elevated close to the shore (Fig. 2). The amplitude in density variation also decreased at M300, located at the sharp turn of the canyon, perhaps because of energy loss in the internal wave.

Fig. 8 shows the empirical orthogonal function (EOF) analysis of the CTD density profiles from stations M444, M300, and M260. The numbers of casts analyzed were 16, 42, and 23, respectively, from these three stations (some shallow deployments were ignored in EOF analysis). The first mode accounted for about 70% of the total variance, and the second mode was relatively small. The time series of the first-mode structure indicated semidiurnal (M_2) variations for all three experiments. The maximum variation of vertical structure occurred at 160 m at the deep station (M444) and decreasing to 90 m at the shallow station (M260), indicating that the maximum amplitudes followed the rising pycnocline toward the canyon head. The amplitude of the first mode indicated vertical displacements consistent with the wave beam scenario revealed by the harmonic analysis of the ADCP data (Fig. 5). Mode 2 had a large amplitude variation at 50 m at the shallow station (M260). This may be explained by the internal wave energy being reflected back over steep topography (i.e., supercritical bathymetry) (e.g., Munk and Wunsch, 1998).

Fig. 9 shows the semidiurnal (M_2) harmonic fit of density profiles at stations M444, M300, and M260. The numbers of casts are the same as those shown in Fig. 8. The resulting variations of amplitude are similar to those of the first mode of the EOF analysis; the maximum variation occurred at 150 m for the deep station (M444), and decreased to 90 m for the shallow station (M260). The 2 h phase lag between the shallow and deep stations (10 km apart) suggested a phase velocity of 1.4 m s^{-1} eastward. The small phase lag between stations M300 and M260 suggested that a standing wave may have existed at the head of the canyon (approximately 1.5 km, Fig. 2), where the bottom topography becomes supercritical. The variation of amplitude was significantly reduced at M300, probably because of energy loss at the second turn of the canyon. Kunze et al. (2002) indicated that internal tidal energy fluxes can be dramatically reduced at the second bend of MC, even though they managed to overcome the first bend. They suspected that the up-canyon energy flux was lost at the deepest bend, and then regenerated locally. It is interesting that the up-canyon energy loss at KPSC is similar to that at MC that the internal waves managed to overcome the first bend of the canyon but decreased significantly at the second bend. Also, Petruncio et al. (2002) suggested that there could be large portions of lateral transport at the bends of canyons. It appears that the ratio of total internal wave energy to cross-channel width can be a factor in the energy loss which however, will require more detailed study. Radiating beams of internal tide also can become nonlinear as they encounter strong near-surface stratification, leading to turbulence or breaking-up into groups of higher frequency, nonlinear internal waves (New and da Silva, 2002).

5. Discussion

The upper layer flows showed complicated spatial patterns (Fig. 3), yet their phase changes (Fig. 4) indicated basically a barotropic tide with little vertical variation. The orientation of the flow had no clear relationship with the tidal-phase for flows above the canyon rim. We suspect that several factors may be responsible for the small-scale variation of flow patterns in the upper shelf of the KPSC. Petruncio et al. (2002) suggested that there can be lateral transport from depths onto adjacent continental shelves along the canyon rims, causing tidal-period surface currents with small horizontal scales of variability. Such transport may be the reason for the complicated flow pattern above the canyon rim. Klinck (1996) also suggested that an eddy may form at the canyon mouth, due to up-canyon flow induced by the left-bounded currents, as a result of the pressure gradient and Coriolis acceleration. In addition, the barotropic tidal current over the shelf region has a different propagating speed and direction to that of the internal tidal current within the canyon. The flow of the upper layer can be separated from those in the canyon. The details of flow variation above the canyon rim require further study.

The generation of internal tide at the KPSC is unknown. The basic theory for internal tide generation was established decades ago (Baines, 1982). The barotropic tides were known to play a dominant role in driving the internal tides at the topographic relief or shelf break (Hotchkiss and Wunsch, 1982; Kunze et al., 2002). Egbert and Ray (2000), based on the observed spatial distribution of tidal energy, suggested that tidal flows over rough topography play a significant role for scattering into internal tides. Petruncio et al. (1998), applying ray-tracing techniques, showed that the two ridges at the outer edge of MC are near-critical (bottom slope) for the M_2 frequency and thus are favorable for internal tide

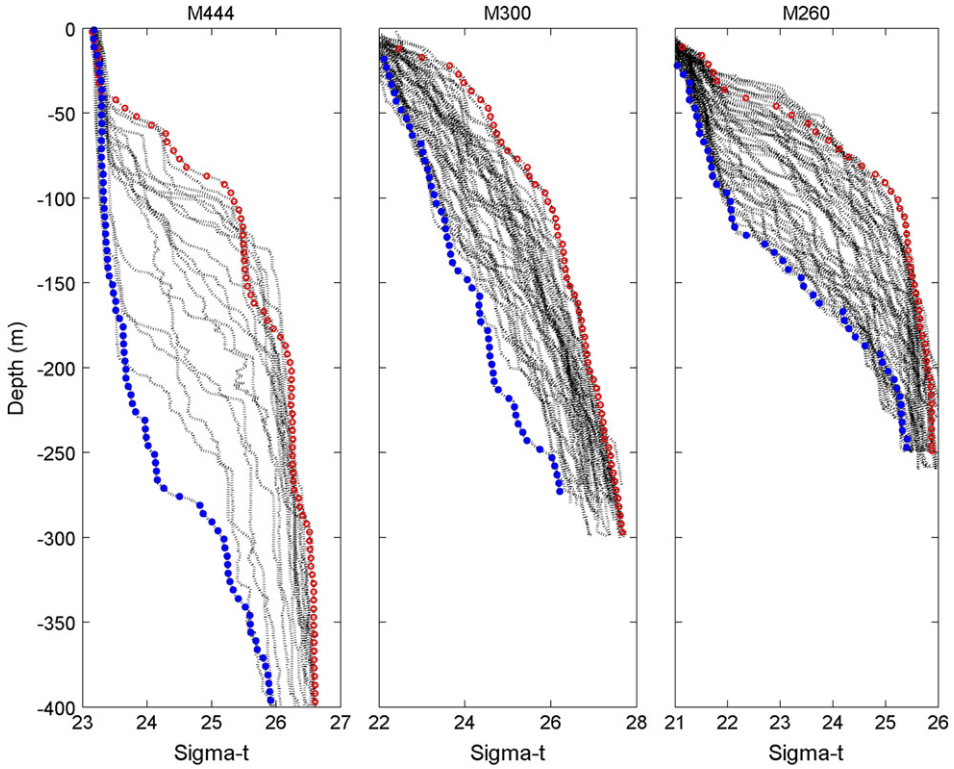

Fig. 7. Hourly density profiles at stations M444, M300, and M260. The minimum (circles) and maximum (dots) depths of the thermocline are illustrated. The vertical displacements of isotherms were about 200, 160, and 140 m from the deep station to the shallow station.

generation. Laurent et al. (2003) showed that internal tides can be generated at knife-edge ridge and abrupt step topography. It is likely that the large topographic variation, both in width and depth, at the mouth of the KPSC is the source of the internal tide. On the other hand, Kunze et al. (2002) suspected that the likely candidates in MC were local internal tide generation along the canyon axis and over rough topography. Based on numerical modeling simulations, Petruncio et al. (2002) showed that the internal tide generation can

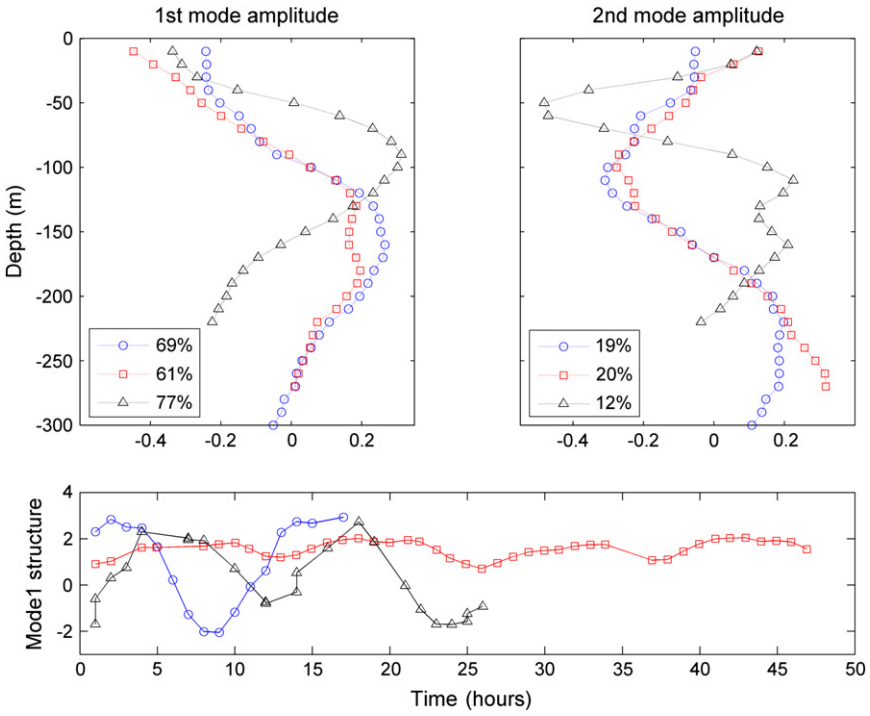

Fig. 8. Empirical orthogonal function (EOF) analysis of CTD profiles at station M444 (circle), M300 (square), and M260 (triangle). Lower left insets in the top two plots indicate the portion of the variance accounted for by the EOF amplitude at each station. The first mode accounts for about 70% of the total variance, whereas the second mode signal is relatively small. Maximum variation occurs at 160 m at the deep station (M444) and decreases to 90 m at the shallow station (M260). Mode 2 has a large value at 50 m at the shallow station (M260). The time series (bottom) of the first mode structure indicates semidiurnal (M_2) variations for all three experiments.

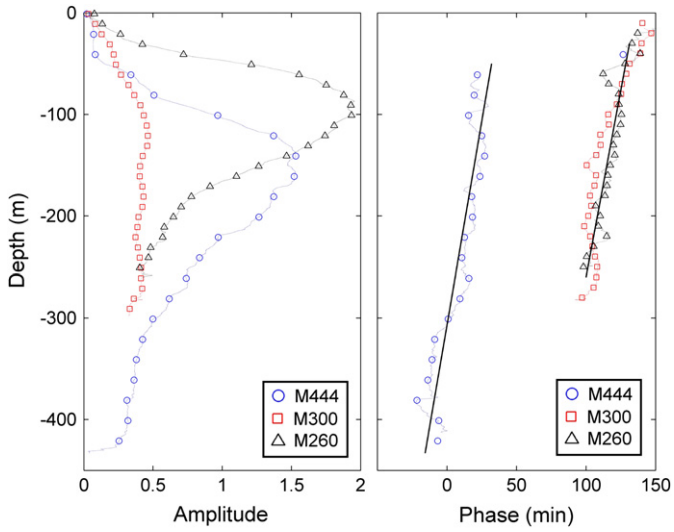

Fig. 9. Harmonic fit of CTD profiles at the M_2 semidiurnal period, with the same data set as shown in Fig. 8. The amplitude is similar to that of the first mode of the empirical mode function analysis. The phase at the shallow station (M260) lags that of the deep station (M444) by 2 h.

occur at the foot, floor, and rims of MC. The bends and rough bottom along the KPSC may also favor generation of internal tide. Field observation coupled with numerical modeling will be needed for future study in KPSC.

During our experiments, many fishing boats trawling for cherry shrimp (*Sergia lucens* Hansen) were seen at the bank of the KPSC (Fig. 10). Shrimp harvesting is an important part of the local economy. The shrimp has a crunchy texture and tasty meat. These shrimp were seen underwater dancing and flying with glowing bodies like cherry petals flying in the air. Yu et al. (1993), using a remotely operated vehicle (ROV), observed high-density burrows on the canyon walls. The openings of most burrows had distinct edges, as if they were occupied by shrimp (Fig. 10). The fishing boats trawling at the northern flank of the canyon during the flood currents are a heritage from generations of field experience (fishermen knew exactly where and when to trawl without scientific knowledge). Generally, trawls are conducted in the upper 150 m of water, which includes the deep "scattering" layer (about 70–90 m in this region, as shown in Fig. 2, a rich zone of living organisms that scatter or reflect sound waves). There were a few studies explaining the link between the internal waves (internal tide) and the biology (fisheries). For example, Wolanski et al. (2004) suggested that internal waves and associated large temperature fluctuations, enhanced by a complex bathymetry, may responsible for the high biodiversity of Palau coral reefs, as well as their temporal and spatial variability. In the Ribbon Reefs in the northern Great Barrier Reef of Australia, Wolanski et al. (1998) indicated that the jet-driven upwelling and tidal jet-vortex pair system may enrich the productivity of the Alga *Halimeda* and even sustain the black marlin stock concentrated in the area of the Ribbon Reefs.

During the flood, currents below the canyon rim are moving essentially all in the landward direction in KPSC (Fig. 4). This indicates that there must be lateral transports across the rim. Unfortunately, our data are not adequate to estimate the longitudinal divergence of along-canyon transport, due to lack of velocity measurements in the lowest 100 m of water column. We suspect though the lateral transports are not too substantial as the internal tidal velocities tend to increase toward the canyon head (Fig. 5). Near the canyon head, however, the channel becomes much narrower, yet the current speeds are at maximum (Fig. 5). Strong convergence must occur, that is, part of the incoming cold water has to be pumped out of the canyon near the head. Then, cherry shrimps either take advantage of the strong upwelled nutrient-rich water or they are simply being forced out of the burrows by turbulent currents. One remaining interesting question is why the trawls are concentrated on the northern flank. We suspect there is

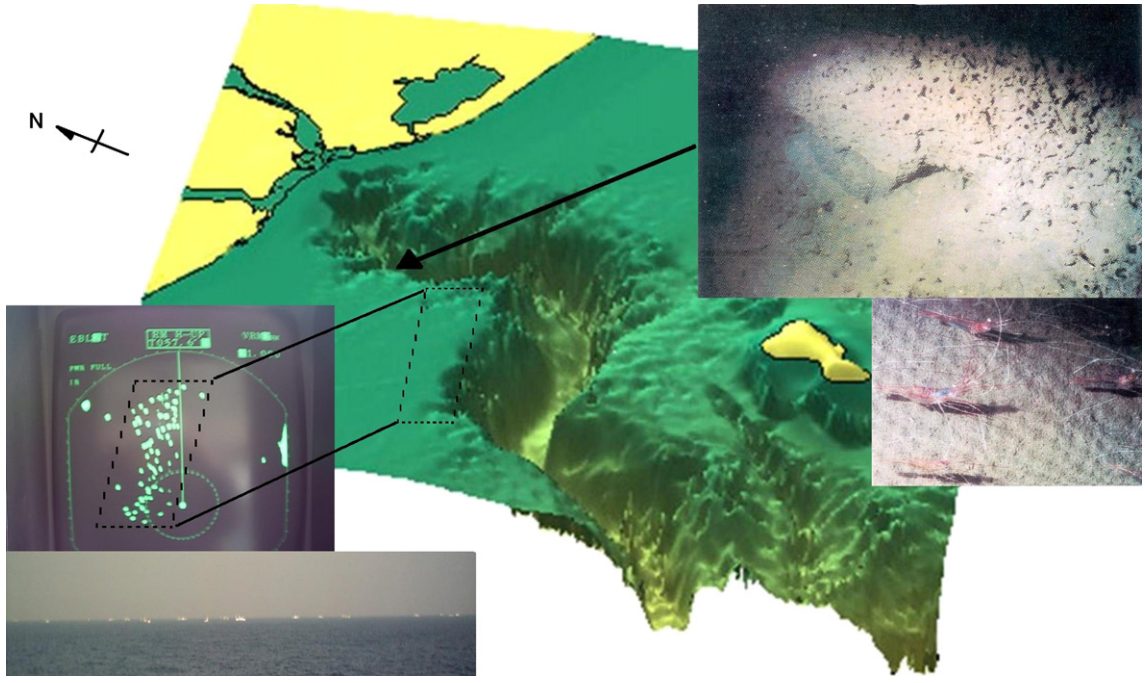

Fig. 10. During field experiments, many fishing boats (radar image and photo) trawling for cherry shrimp were observed at the bank of the KPSC. ROV observations (Yu et al., 1993) revealed high densities of burrows (upper right inset) along the steep slopes of the canyon wall; the openings of most burrows had distinct edges, as if they were occupied by cherry shrimp.

a strong secondary circulation associated with the sharp bending of the canyon axis that vertical motion is much stronger to the left (north) of the flood current. Secondary circulation around headland is well known in shallow estuaries (e.g., Chant and Wilson, 1997). It is likely that the centrifugal acceleration plays an even more prominent role in narrow canyons. In the end, scientists might also learn something from the fishermen.

6. Conclusion

This study provides estimates of internal tidal amplitude, phase speed, and water displacement, based on measurements of velocity and density profiles along the main axis of Kaoping Canyon. Analyses of the temporal and spatial data lead us to the following conclusions. (1) The velocity data showed two flow layers separated, roughly, at the rims of the canyon. (2) Flows in the canyon showed a dominant internal tide. The velocity amplitudes increased with depth, and toward the canyon head. The estimated internal tidal-phase velocity was about 1.5 $m\,s^{-1}$. (3) Analyses of hydrographic profiles and velocity data suggest that cold bottom water moved up-canyon during flood, and warm water drained out of the canyon during ebb. (4) The internal tide-induced isotherm displacement was over 200 m, which might play an important role in mixing, leading to offshore transport of river-discharged materials. (5) At the head of the canyon the small phase lag of semidiurnal internal tide and the large mode 2 amplitude from EOF analysis of CTD data suggested the existence of a standing wave where the bottom topography becomes supercritical.

Acknowledgments

We thank Dr. E. Wolanski, and two anonymous reviewers for helpful comments. Dr. D.P. Wang provided edits to improve the manuscript. Ms. Y.Z. Lin helped collate the data. Water depth data were provided by the Ocean Data Bank, Taipei. Tidal data were collected by the Central Weather Bureau of Taiwan. This work was supported by the National Science Council, Taiwan, and the Aim for Top University Plan.

References

Allen, G.L., Simpson, J.H., 1998. Reflection of the internal tide in Upper Loch Linnhe, a Scottish fjord. Estuarine Coastal and Shelf Science 46, 683–701.
Baines, P.G., 1982. On internal tide generation models. Deep-Sea Research 29, 307–338.
Chant, R., Wilson, R., 1997. Secondary circulation in a highly stratified estuary. Journal of Geophysical Research 102 (C10), 23207–23215.
Egbert, G.D., Ray, R.D., 2000. Significant dissipation of tidal energy in the deep ocean inferred from satellite altimeter data. Nature 405, 775–778.
Gill, A.E., 1982. Atmosphere-Ocean Dynamics. Academic Press.
Hotchkiss, F.S., Wunsch, C.H., 1982. Internal waves in Hudson Canyon with possible geological implications. Deep-Sea Research 29, 415–442.
Huh, C.A., Lin, H.L., Lin, S.W., Huang, Y.W., 2008. Modern accumulation rates and a budget of sediment off the Gaoping River, SW Taiwan: a tidal and flood dominated depositional environment around a submarine canyon. Journal of Marine Systems, in press.
Jeng, W.L., Wang, J., Han, B.C., 1996. Coprotanol distribution in marine sediments off southwestern Taiwan. Environmental Pollution 94 (1), 47–52.
Klinck, J.M., 1996. Circulation near submarine canyon: a modeling study. Journal of Geophysical Research 101 (C1), 1211–1223.
Kunze, E., Rosenfeld, L.K., Carter, G.S., Gregg, M.C., 2002. Internal waves in Monterey Submarine Canyon. Journal of Physical Oceanography 32, 1890–1913.
Laurent, L.S., Stringer, S., Garrett, C., Perrault-Joncas, D., 2003. The generation of internal tides at abrupt topography. Deep-Sea Research 50, 987–1003.
McPhee-Shaw, E.E., Sternberg, R.W., Mullenbach, B., Ogston, A.S., 2004. Observations of intermediate nepheloid layers on the northern California continental margin. Continental Shelf Research 24, 693–720.
Munk, W., Wunsch, C., 1998. Abyssal recipes II: Energetics of tidal and wind mixing. Deep-Sea Research 45, 1977–2010.
New, A.L., da Silva, J.C.B., 2002. Remote-sensing evidence for the local generation of internal soliton packets in the central Bay of Biscay. Deep-Sea Research 49, 915–934.
Petruncio, E.T., Rosenfeld, L.K., Paduan, J.D., 1998. Observations of the internal tide in Monterey Canyon. Journal of Physical Oceanography 28, 1873–1903.
Petruncio, E.T., Paduan, J.D., Rosenfeld, L.K., 2002. Numerical simulations of the internal tide in a submarine canyon. Ocean Modelling 4, 221–248.
Wang, Y.H., Chiao, L.Y., Lwiza, K.M.M., Wang, D.P., 2004. Analysis of flow at the gate of Taiwan Strait. Journal of Geophysical Research 109. C02025, doi:10.1029/2003JC001937.
Wolanski, E., Drew, E., Abel, K.M., O'Brien, J., 1998. Tidal jets, nutrient upwelling and their influence on the productivity of the alga *Halimeda* in the Ribbon Reefs, Great Barrier Reef. Estuarine Coastal and Shelf Science 26, 169–201.
Wolanski, E., Colin, P., Naithani, J., Deleersnijder, E., Golbuu, Y., 2004. Large amplitude, leaky, island-generated, internal waves around Palau, Micronesia. Estuarine Coastal and Shelf Science 60, 705–716.
Xu, J.P., Noble, M., Eittreim, S.L., Rosenfeld, L.K., Schwing, F.B., Pilskaln, C.H., 2002. Distribution and transport of suspended particulate matter in Monterey Canyon, California. Marine Geology 181, 215–234.
Yu, H.S., Auster, P.J., Cooper, R.A., 1993. Surface geology and biology at the head of Kaoping Canyon off southwestern Taiwan. Terrestrial Atmospheric and Oceanic Sciences 4, 441–455.